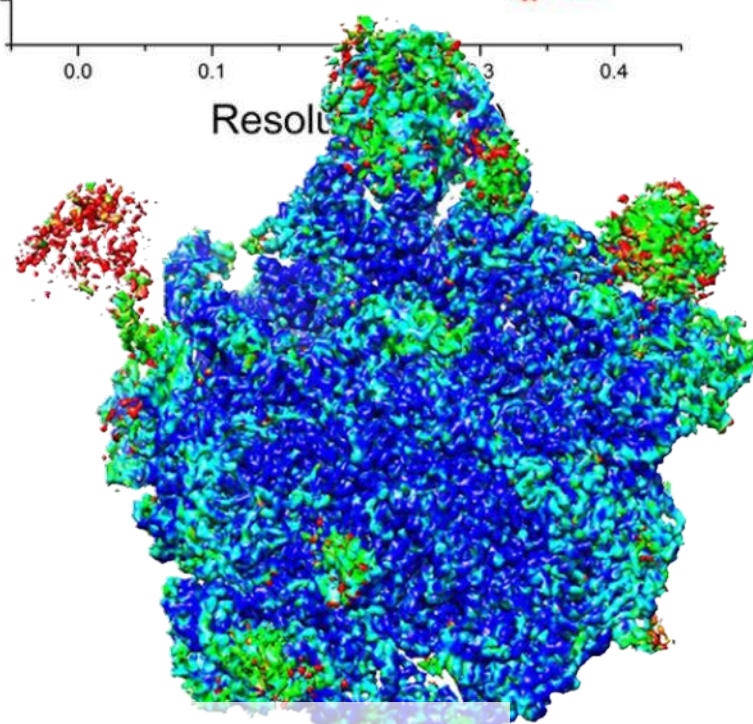
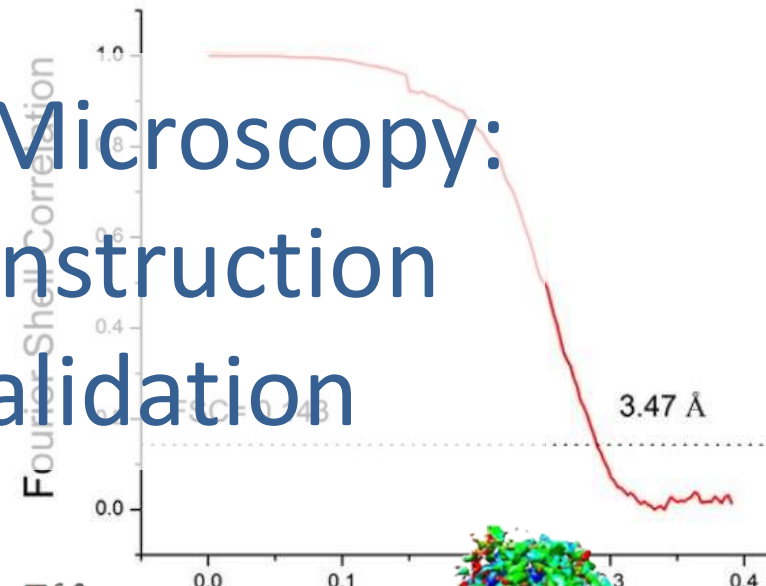
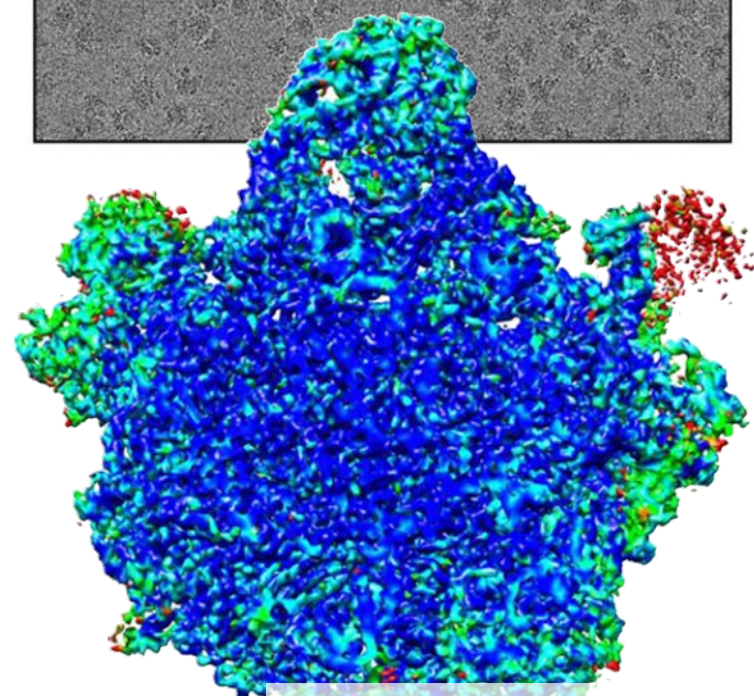


# Electron Microscopy: 3D reconstruction and validation

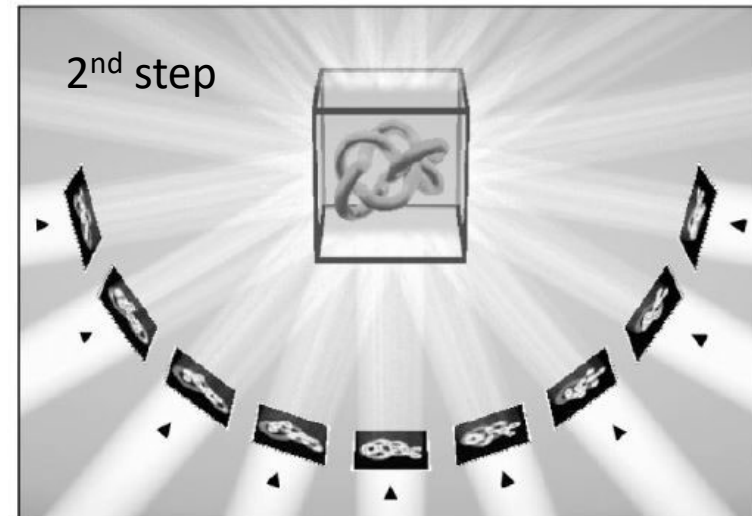
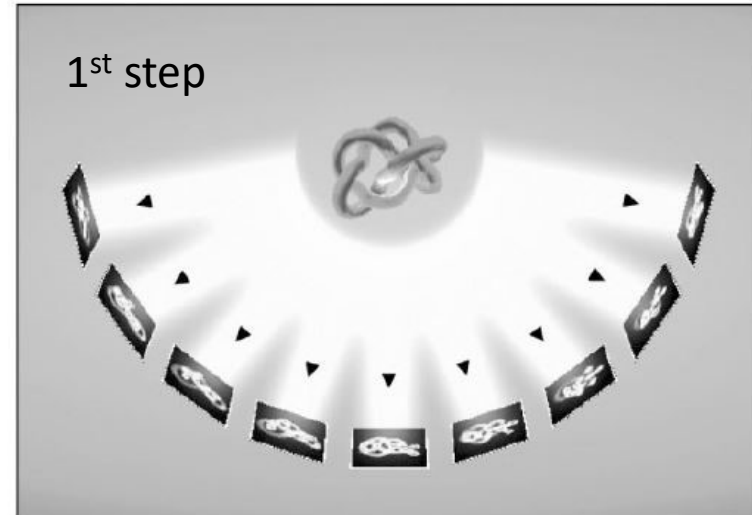
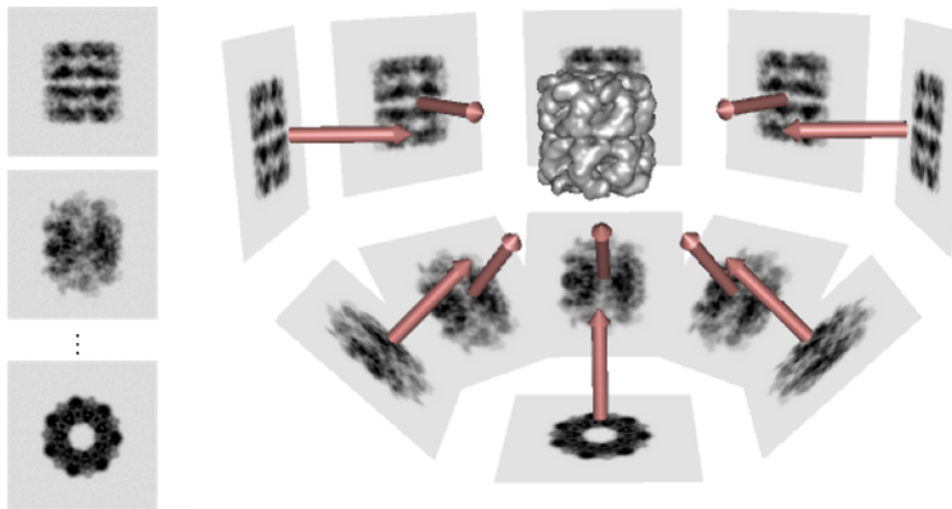


Corso di Biocristallografia e Microscopia Elettronica

rdezorzi@units.it

# 3D reconstruction

Reconstruction is the process to obtain from 2D images of particles the 3D map of electrostatic potential (volume of the object)



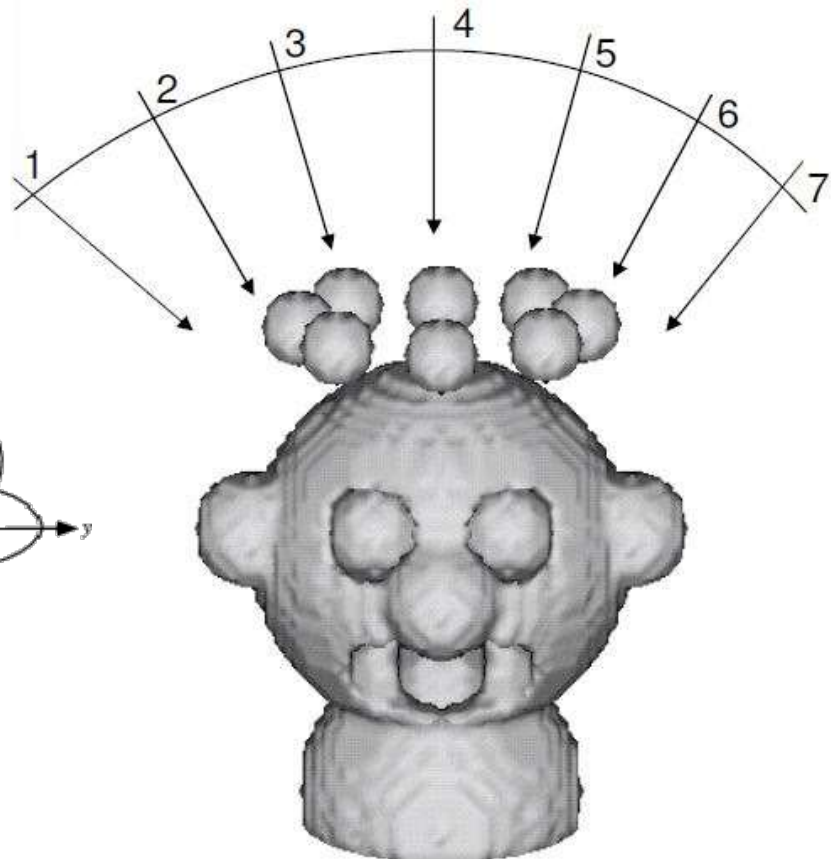
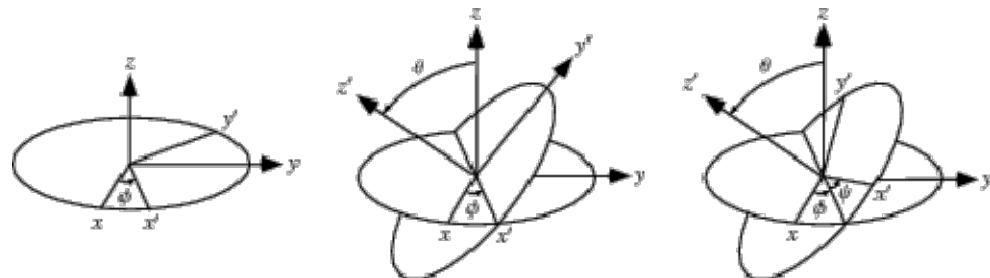
The reconstruction is carried on in 2 steps:

1. Determination of the Euler angles of each particle image
2. Reconstruction of the volume from the images with assigned angles

# Some basic ideas...

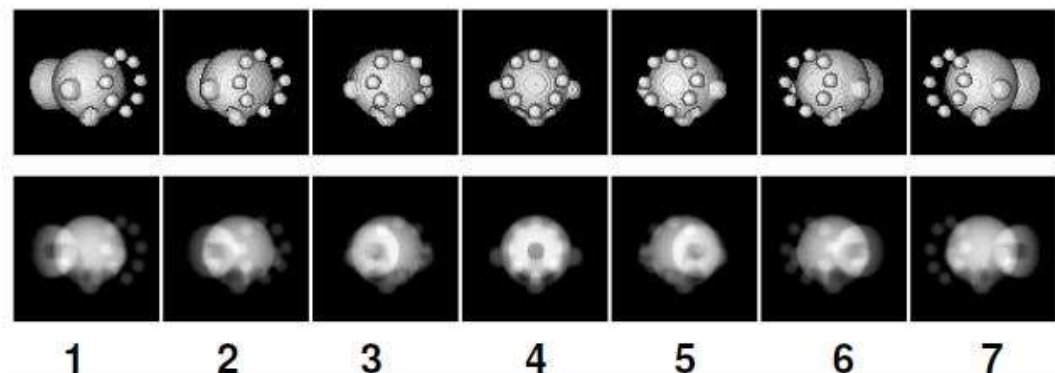
## Euler angles:

Rotation angles of each particle compared to the incident electron beam, determining the projection of particles in a different orientation



## Projection:

The image of the particle obtained from the micrographs is NOT just the shape of the molecule, but the **projection of the electrostatic potential** of the protein: features are present in the interior of particles.



# Step 1: Euler angles determination

For reconstruction, projections of the particles in different orientations are required.

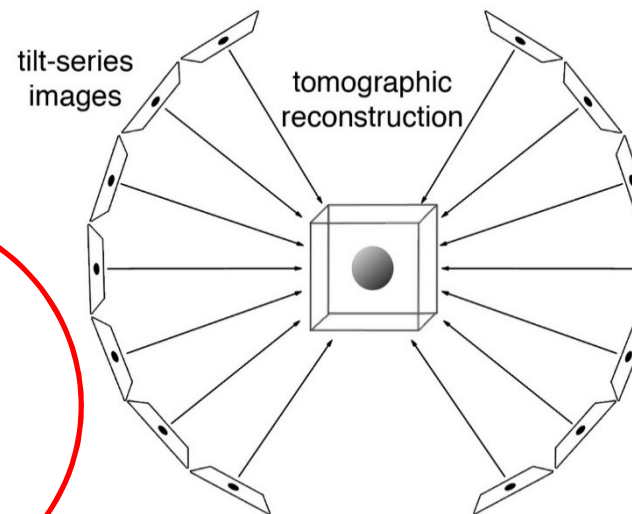
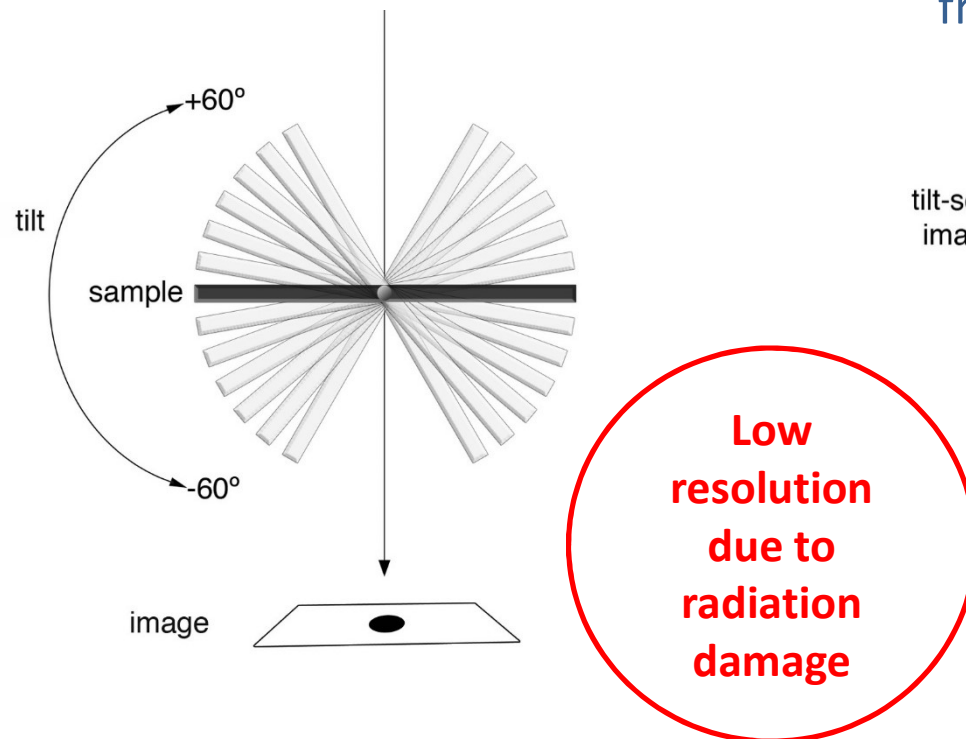
To each particle orientation (Euler angles) must be assigned.

1

Reconstruction from many images of the same particle in different orientations:

**ELECTRON TOMOGRAPHY**

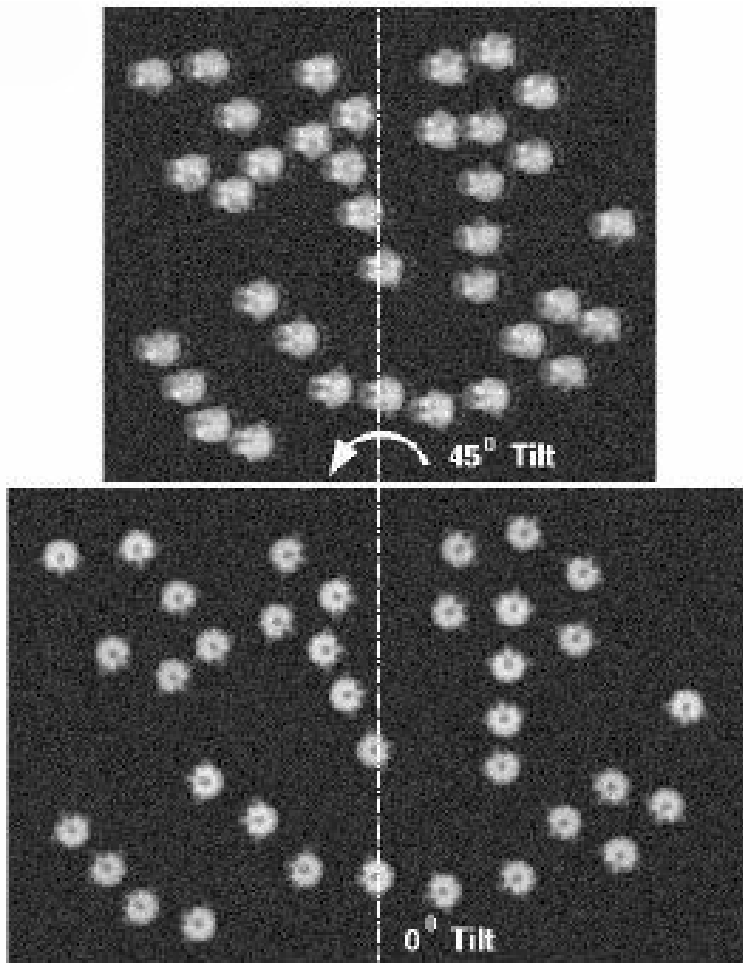
Relative orientation of images is known from the experiment: tilt angle



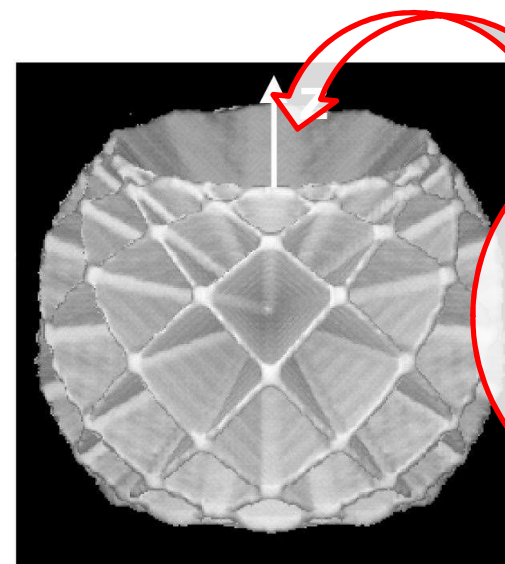
# Random Conical Tilt Method

For grids with preferential orientation  
(e.g. negative staining)

Collection of 'tilt pairs' – 45° and 0° tilt

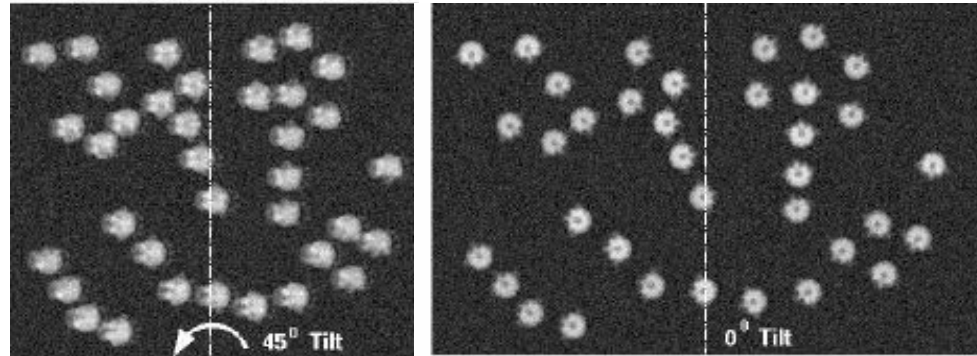


Particles selected  
from tilt pairs  
**Euler angles** are  
known from the tilt  
axis&angle



Missing  
cone causes  
distortions  
in the  
structure

1. Data collection: collect a  $45^\circ$ -tilted image

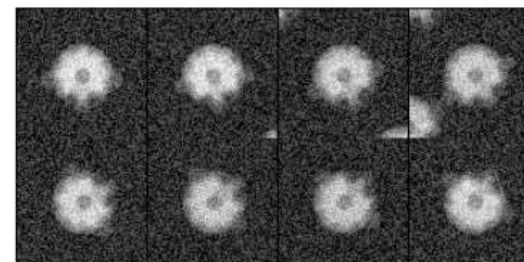
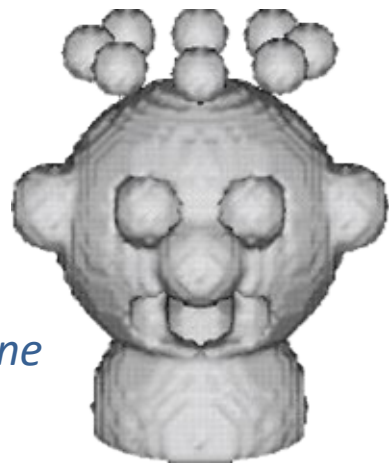


2. Data collection: on the same grid position, collect untilted image

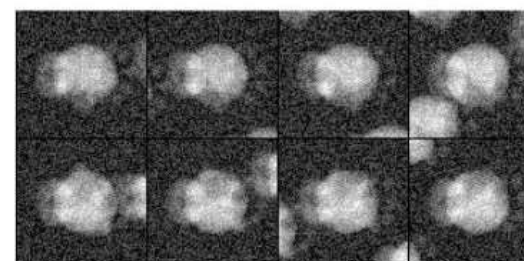
*$0^\circ$ -tilt images will not be used for final 3D reconstruction, but only for identification of Euler angles.*

3. Interactive windowing of particles in the two micrographs. Centering and masking.

*At  $0^\circ$  tilt, projections of the same object are identical except for in-plane rotation (Euler angle  $\varphi$ ). At  $45^\circ$ , particles are different.*



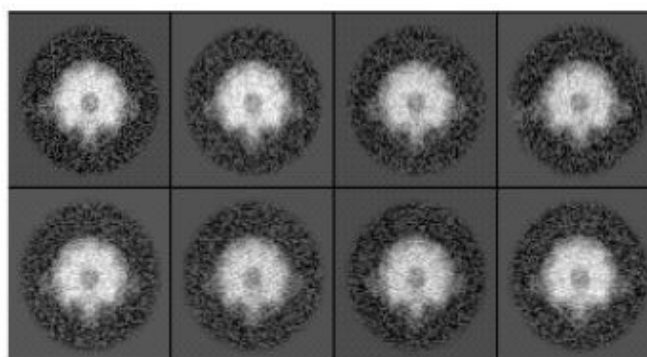
$0^\circ$



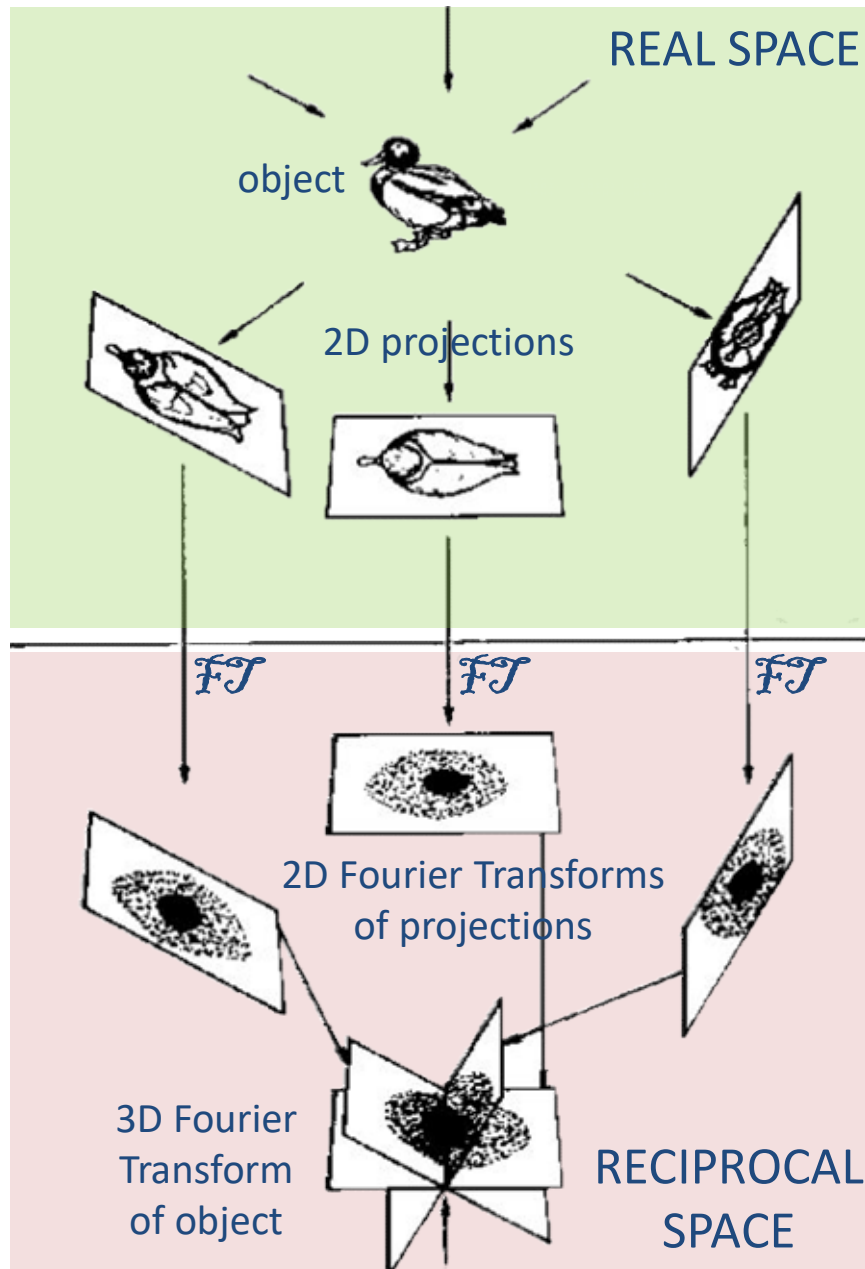
$45^\circ$

4. Alignment and classification of particles from  $0^\circ$ -tilt to identify  $\varphi_i$ .

*Other Euler angles identified from tilt geometry. Determination of correct tilt geometry is crucial!*



5. Scaling of tilted data.



## Projection Theorem (or Radon's Theorem)

In reciprocal space, every 2D projection of a 3D object corresponds to a 2D central section of the 3D Fourier transform of the object.

The central section obtained from the Fourier transform of a projection is orthogonal to the direction of the projection.

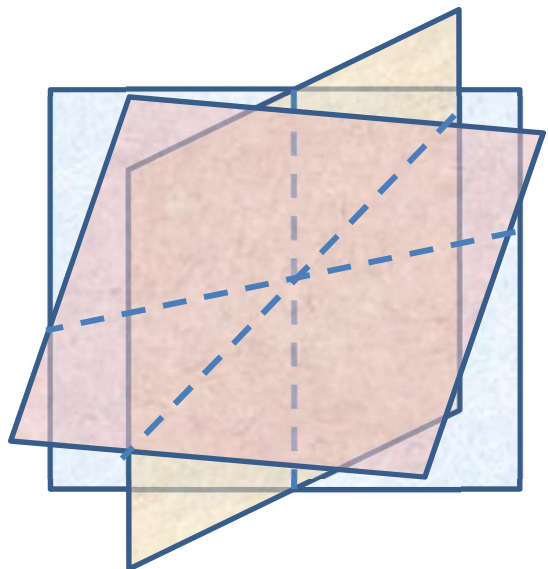
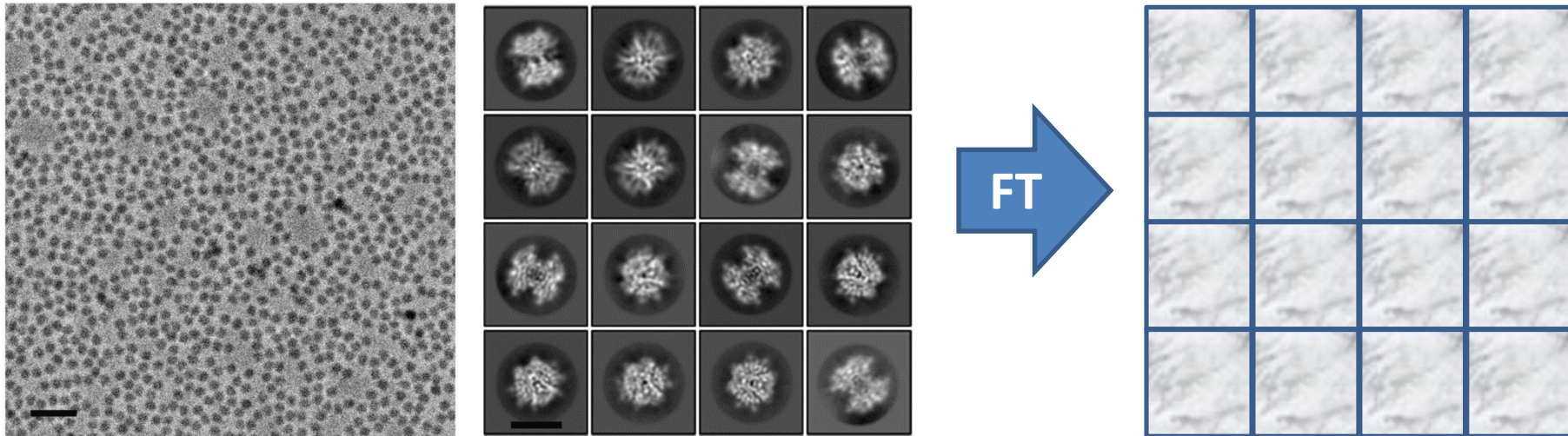
Considering this theorem, the reconstruction of the object from 2D projections is possible, but...

- (1) How many images are required?  
What is the necessary coverage of the reciprocal space?
- (2) Would reconstruction be unique?

3

## Common-Lines Method

If images of particles are collected in random orientations (e.g. cryo-EM):



Considering the projection theorem, each FT of a projection includes the center of the Fourier space.

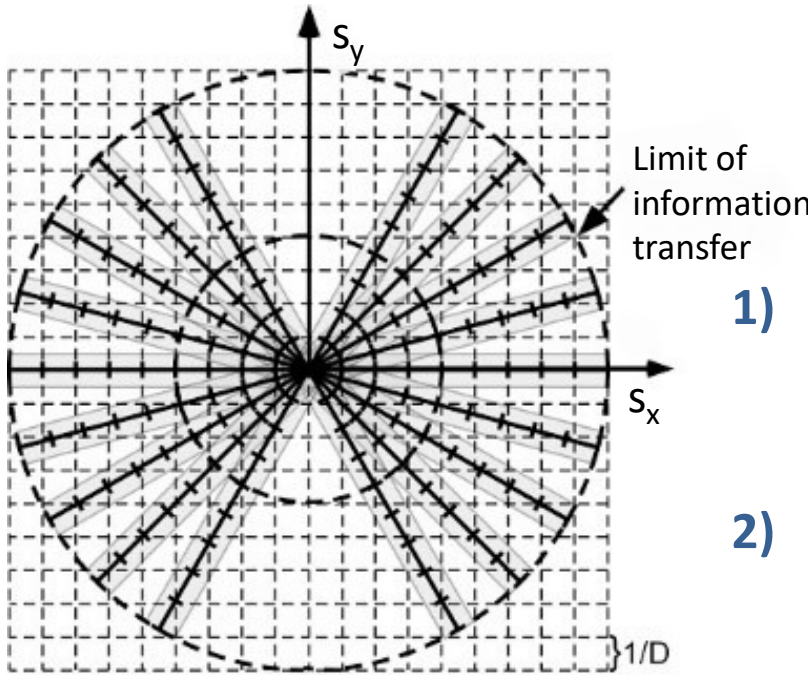
Two FTs of different projections share a **common line**.

Addition of a third projection allows to identify common lines between this and the previous projections...

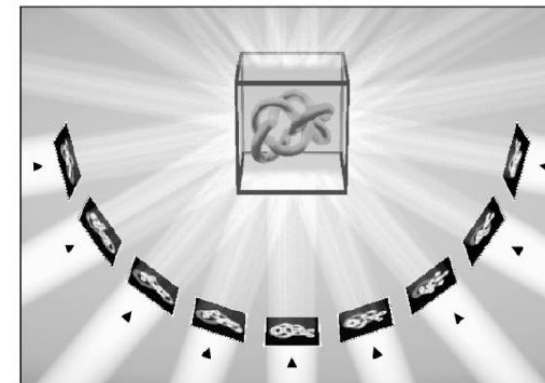
and to determine relative **Euler angles**.

## Step 2: Reconstruction

- Can we reconstruct the initial volume with an uneven angular distribution?
- How does noise affect the reconstruction?
- How to incorporate constraints?



Sampling in Fourier space is not homogeneous: high frequencies are less sampled than low frequencies, causing reduction of resolution.



### Methods:

- 1) **Weighted back projection:** reconstruction of the volume in real space, using a function that inverts the projection.
- 2) **Fourier reconstruction methods:** reconstruction in reciprocal space, from the Fourier transforms of each image aligned by Euler angles
- 3) **Simultaneous Iterative Algebraic Reconstruction Method (SIRT)**

# CTF correction

CTF correction can be applied:

- On single raw images or micrographs, but this approach is limited due to SNR of single images
- Application of CTF correction after reconstruction, by dividing particles into defocus groups based on original micrographs. (But defocus groups should have a small step to avoid errors in CTF correction that would decrease resolution.)
- Simultaneous CTF correction and reconstruction, using iterative methods... see next slides (Relion, Freealign...)

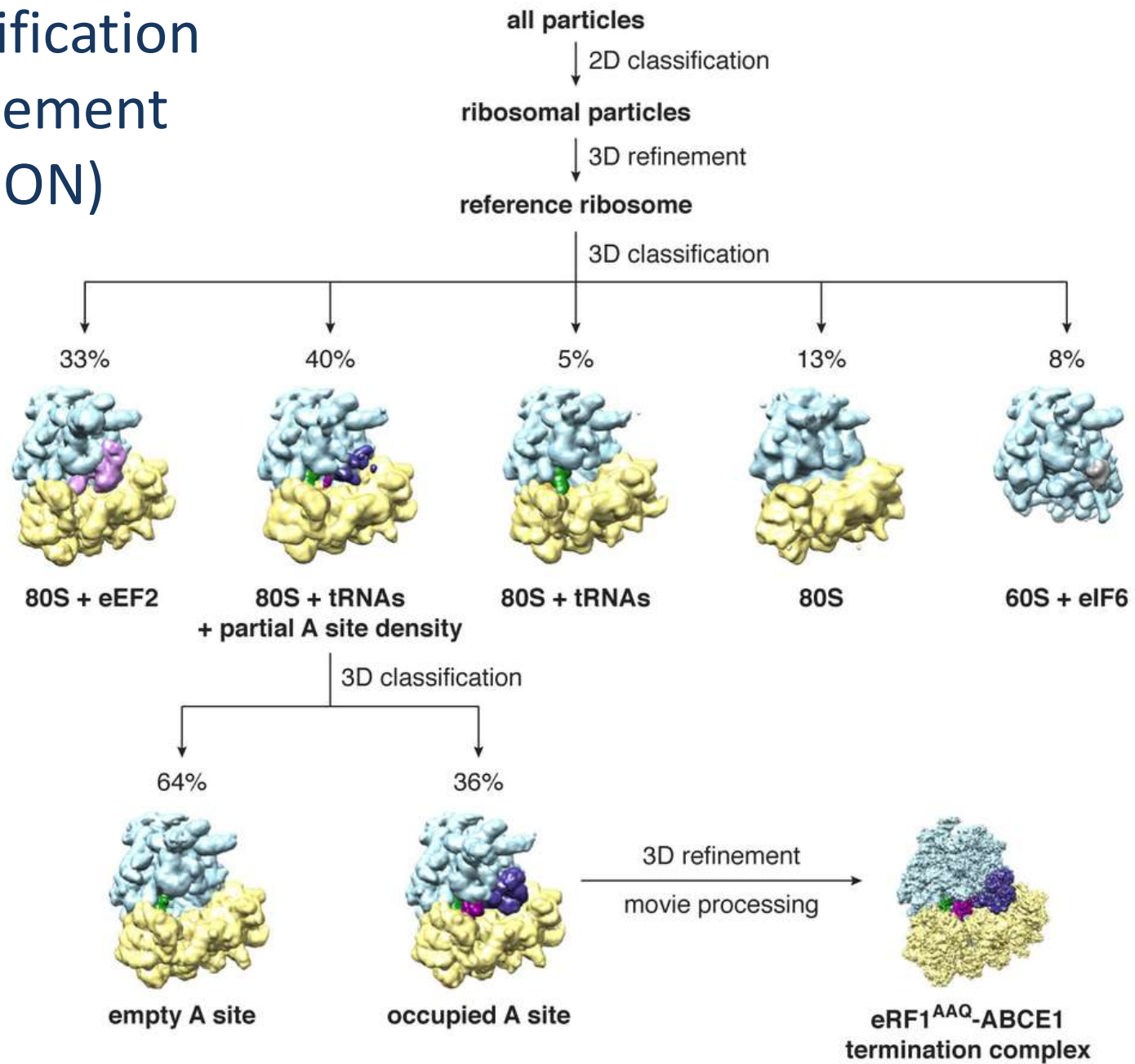
\* For Random Conic Tilt approach, additional problem due to different defocus of particles in 45°-tilted micrographs (according to position of the particle in the micrograph...)

# Heterogeneity

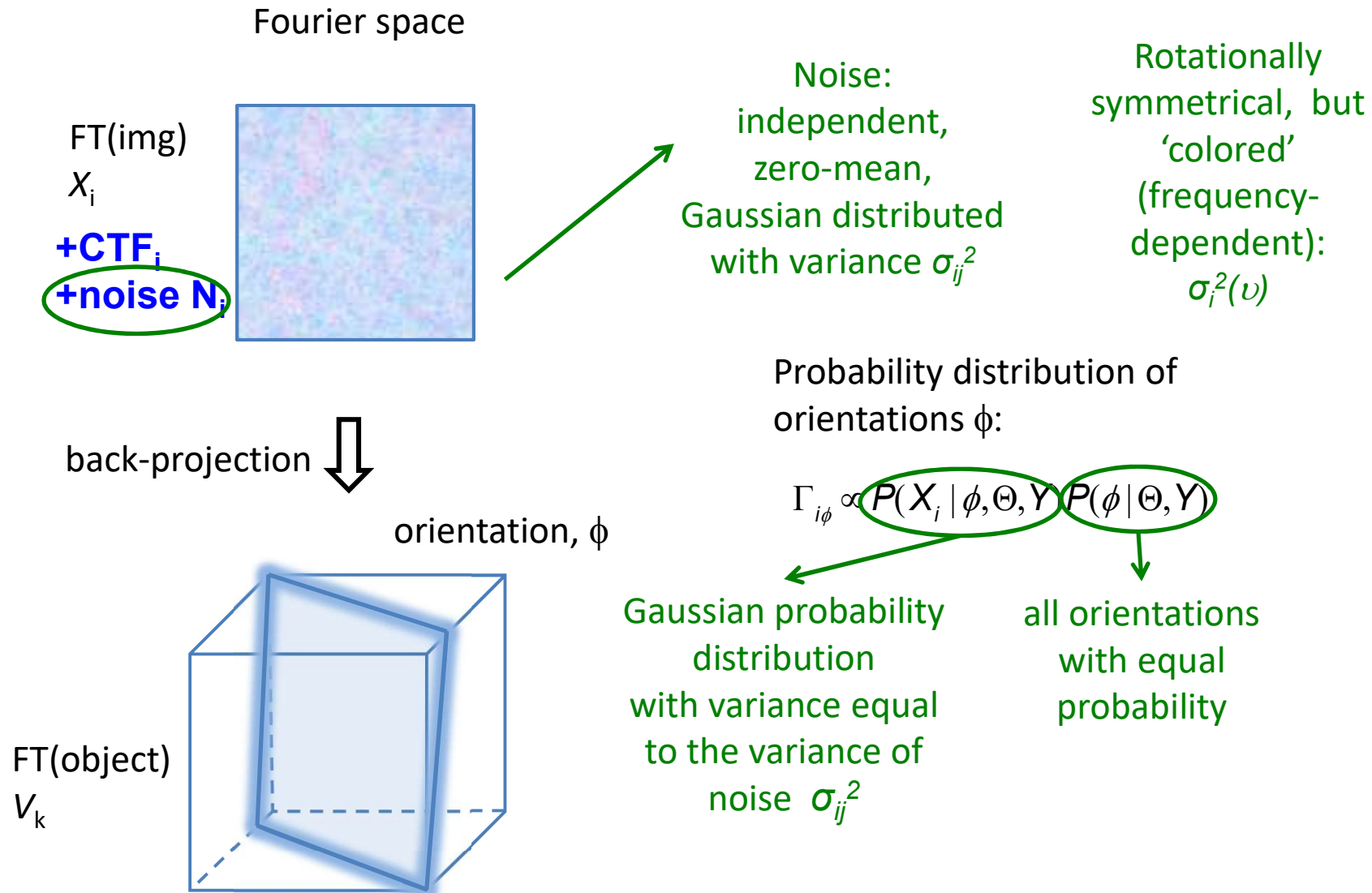
Is it possible to separate images from different conformations of the protein/complex in the sample?

# 3D Classification & Refinement (RELION)

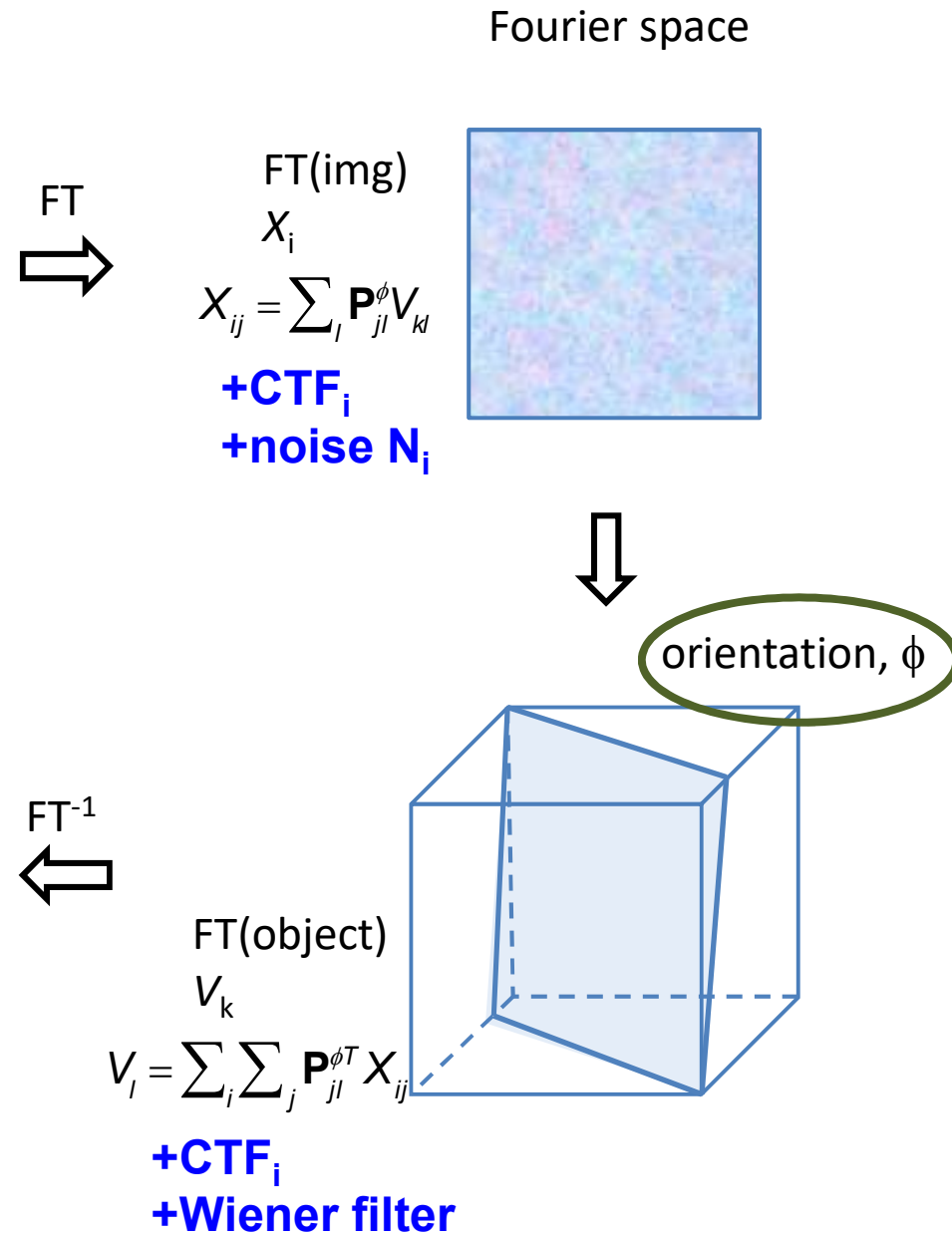
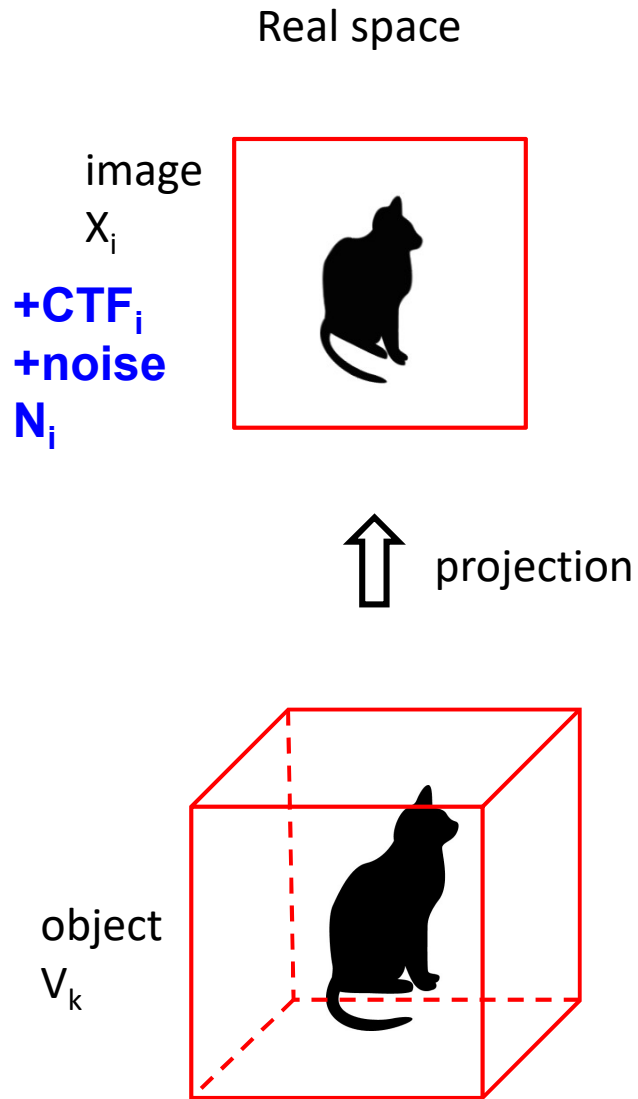
Classification based on a 3D model:  
previous structure obtained from X-ray crystallography, Negative Staining EM, ab initio cryo-EM reconstruction



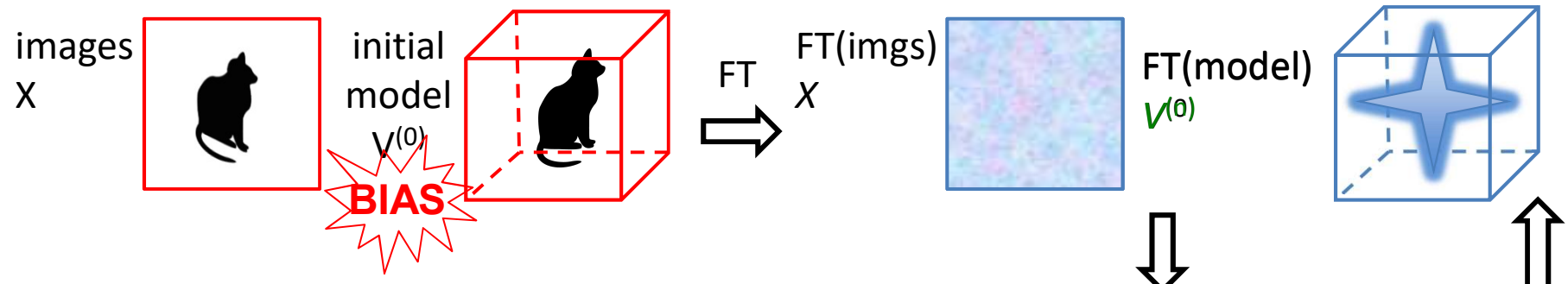
# Statistical approach



# Relion algorithm



# Iterative algorithm



$$\Gamma_{i\phi}^{(1)} \propto \prod_j \frac{1}{2\pi\sigma_{ij}^2} \exp\left(\frac{|X_{ij} - CTF_{ij} \sum_l \mathbf{P}_{jl}^\phi V_l^{(0)}|^2}{-2\sigma_{ij}^2}\right)$$

$$V_l^{(1)} \propto \sum_{i\phi} \left\{ \int \left[ \Gamma_{i\phi} \cdot \left( \sum_j \mathbf{P}_{jl}^{\phi T} X_{ij} \right) \right] d\phi \right\}$$

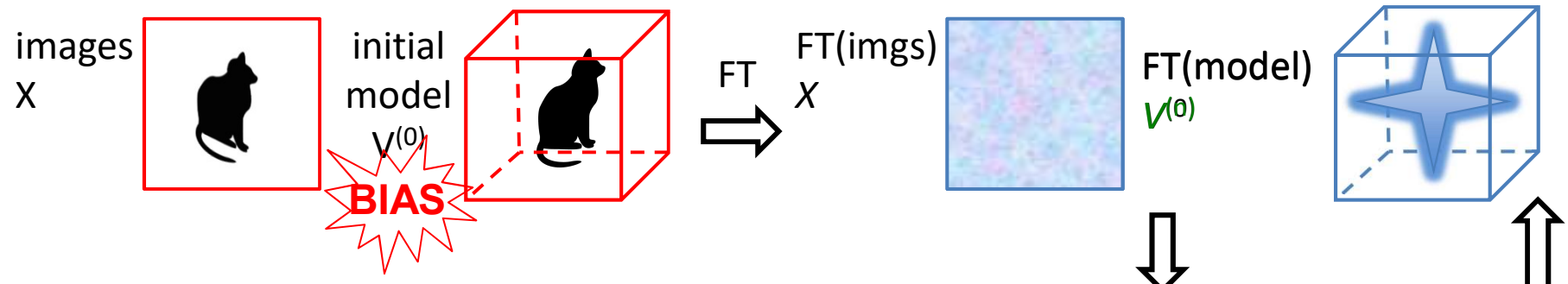
$$\sigma_{ij}^{2(1)} = \frac{1}{2} \int_{\phi} \Gamma_{i\phi}^{(1)} \cdot \left| X_{ij} - CTF_{ij} \left( \sum_l \mathbf{P}_{jl}^\phi V_l^{(1)} \right) \right|^2 d\phi$$

$$\tau_l^{2(1)} = \frac{1}{2} |V_l^{(1)}|^2$$

Calculate:

- Probability distribution of orientations,  $\Gamma_{i\phi}^{(1)}$ , by comparing FT of images with slices of the Fourier space, weighted by the noise of each image.
- The new model,  $V^{(1)}$ , by back-projecting each image, with orientations weighted by their probability (and with an additional Weiner filter).
- The variance of the noise,  $\sigma_{ij}^{2(1)}$ , and the variance of the signal,  $\tau_l^{2(1)}$  (used in the Weiner filter).

# Iterative algorithm



$$\Gamma_{i\phi}^{(n+1)} \propto \prod_j \frac{1}{2\pi\sigma_{ij}^{2(n)}} \exp \left( \frac{\left| X_{ij} - CTF_{ij} \sum_l \mathbf{P}_{jl}^\phi V_l^{(n)} \right|^2}{-2\sigma_{ij}^{2(n)}} \right)$$

$$V_l^{(n+1)} \propto \sum_{i\phi} \left\{ \int_{\phi} \left[ \Gamma_{i\phi}^{(n)} \cdot \left( \sum_j \mathbf{P}_{jl}^{\phi T} X_{ij} \right) \right] d\phi \right\}$$

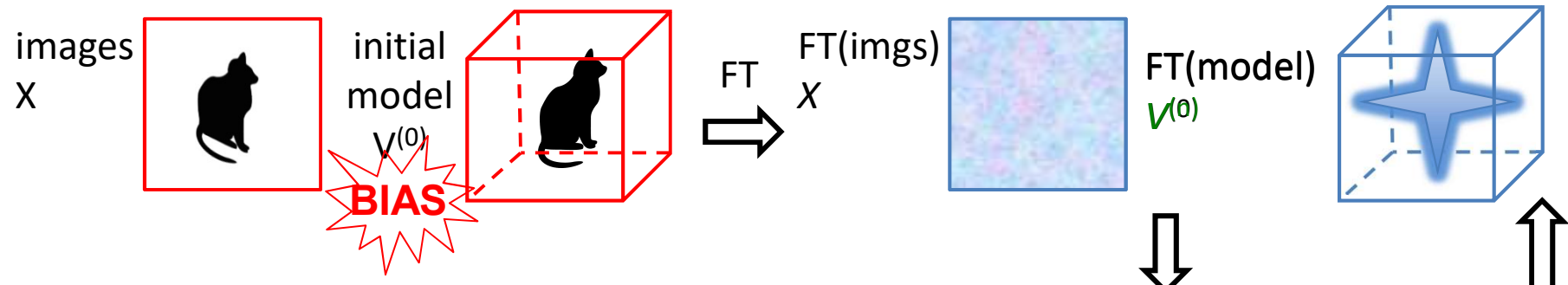
$$\sigma_{ij}^{2(n+1)} = \frac{1}{2} \int_{\phi} \Gamma_{i\phi}^{(n)} \cdot \left| X_{ij} - CTF_{ij} \left( \sum_l \mathbf{P}_{jl}^\phi V_l^{(n)} \right) \right|^2 d\phi$$

$$\tau_l^{2(n+1)} = \frac{1}{2} |V_l^{(n)}|^2$$

Calculate:

- Probability distribution of orientations,  $\Gamma_{i\phi}^{(n+1)}$ , by comparing FT of images with slices of the Fourier space, weighted by the noise of each image.
- The new model,  $V^{(n+1)}$ , by back-projecting each image, with orientations weighted by their probability (and with an additional Weiner filter).
- The variance of the noise,  $\sigma_{ij}^{2(n+1)}$ , and the variance of the signal,  $\tau_l^{2(n+1)}$  (used in the Weiner filter).

# Iterative algorithm



$$\Gamma_{ik\phi}^{(n+1)} \propto \prod_j \frac{1}{2\pi\sigma_{ij}^{2(n)}} \exp\left( \frac{\left| X_{ij} - CTF_{ij} \sum_l \mathbf{P}_{jl}^\phi V_{kl}^{(n)} \right|^2}{-2\sigma_{ij}^{2(n)}} \right)$$

$$V_{kl}^{(n+1)} \propto \sum_l \left\{ \int_\phi \left[ \Gamma_{ik\phi}^{(n)} \cdot \left( \sum_j \mathbf{P}_{jl}^{\phi T} X_{ij} \right) \right] d\phi \right\}$$

$$\sigma_{ij}^{2(n+1)} = \frac{1}{2} \sum_k \left\{ \int_\phi \Gamma_{ik\phi}^{(n)} \cdot \left| X_{ij} - CTF_{ij} \left( \sum_l \mathbf{P}_{jl}^\phi V_{kl}^{(n)} \right) \right|^2 d\phi \right\}$$

$$\tau_{kl}^{2(n+1)} = \frac{1}{2} |V_{kl}^{(n)}|^2$$

Calculate:

- Probability distribution of orientations,  $\Gamma_{i\phi}^{(n+1)}$ , by comparing FT of images with slices of the Fourier space, weighted by the noise of each image.
- The new model,  $V^{(n+1)}$ , by back-projecting each image, with orientations weighted by their probability (and with an additional Weiner filter).
- The variance of the noise,  $\sigma_{ij}^{2(n+1)}$ , and the variance of the signal,  $\tau_{ij}^{2(n+1)}$  (used in the Weiner filter).

3D classification: K different classes, calculates one volume for each class  $V_k^{(n+1)}$

# Structure Validation

Sources of error in Single Particle EM structure determination:

- Particle picking from template can create **model bias** (Einstein from noise)
- **Heterogeneity** of sample can create spurious features
- For NS: artifacts of stain
- Lack of completeness (preferred orientation in NS, but also in cryo)
- **Model bias** in 3D reconstruction
- **Overfitting** (alignment of noise)

**Check samples using NS-EM first, to assess homogeneity of particles**

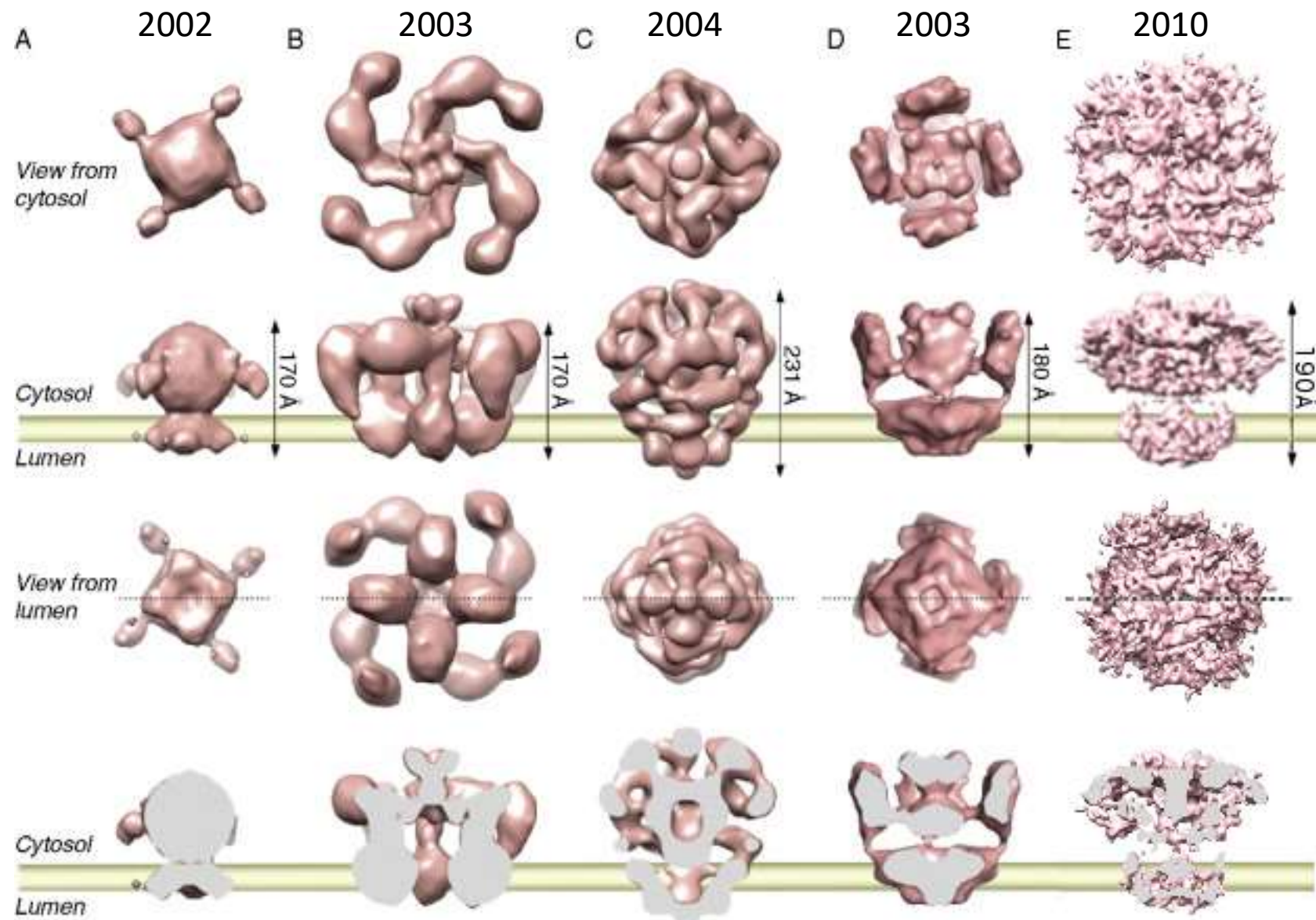
**VALIDATION!!!**

**Check reconstruction results:**

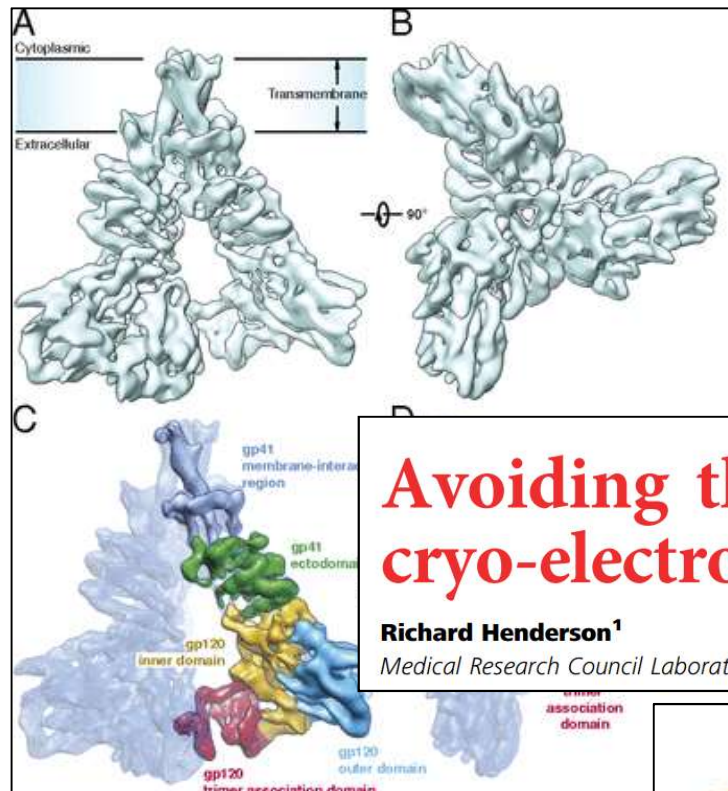
- **Reconstruction with different software**
- **Compare with previous results (MX, NMR, MD, NS-EM, etc.)**
- **Ab initio reconstruction avoids model bias**
- **Validate with tilt pairs**

**Carefully assess RESOLUTION!!**

# Inositol trisphosphate receptor (IP<sub>3</sub>R)



# HIV-1 envelope glycoprotein



**Molecular architecture of the uncleaved HIV-1 envelope glycoprotein trimer**

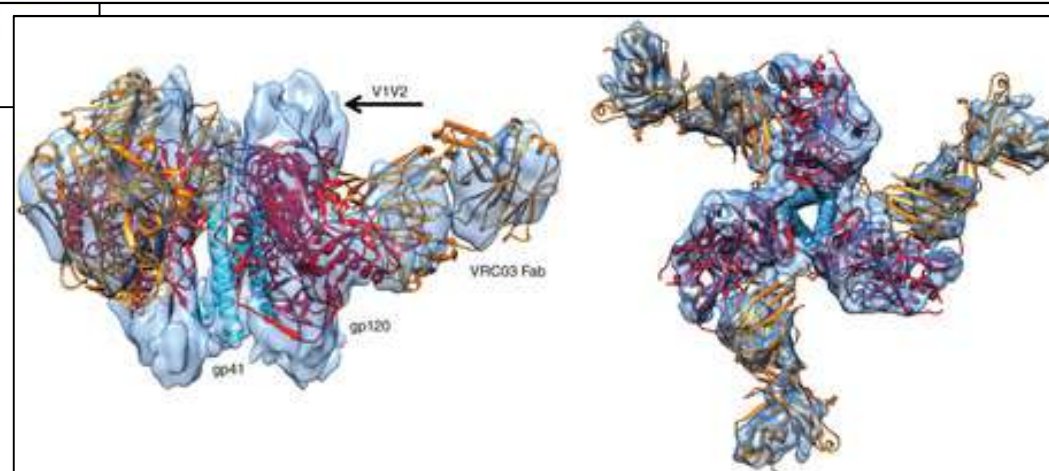
Youdong Mao<sup>a,b,1</sup>, Liping Wang<sup>a,b</sup>, Christopher Gu<sup>a,b</sup>, Alon Herschhorn<sup>a,b</sup>, Anik Désormeaux<sup>c</sup>, Andrés Finzi<sup>c</sup>, Shi-Hua Xiang<sup>d</sup>, and Joseph G. Sodroski<sup>a,b,e,f,1</sup>

<sup>a</sup>Department of Cancer Immunology and AIDS, Dana-Farber Cancer Institute, Boston, MA 02215; <sup>b</sup>Department of Microbiology and Immunobiology, Harvard Medical School, Boston, MA 02115; <sup>c</sup>Centre de Recherche du Centre Hospitalier de l'Université de Montréal, Department of Microbiology and Immunology, Université de Montréal, Montréal, QC, Canada H3A 2B4; <sup>d</sup>Nebraska Center for Virology, School of Veterinary Medicine and Biomedical Sciences, University of Nebraska-Lincoln, Lincoln, NE 68583; <sup>e</sup>Ragon Institute of Massachusetts General Hospital, Massachusetts Institute of Technology, and Harvard, Cambridge, MA 02139; and <sup>f</sup>Department of Immunology and Infectious Diseases, Harvard School of Public Health, Boston, MA 02115

## Avoiding the pitfalls of single particle cryo-electron microscopy: Einstein from noise

Richard Henderson<sup>1</sup>

Medical Research Council Laboratory of Molecular Biology, Cambridge CB2 0QH, United Kingdom



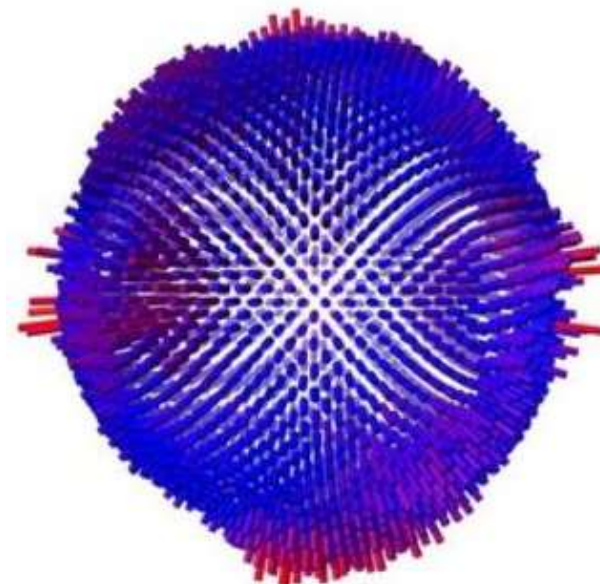
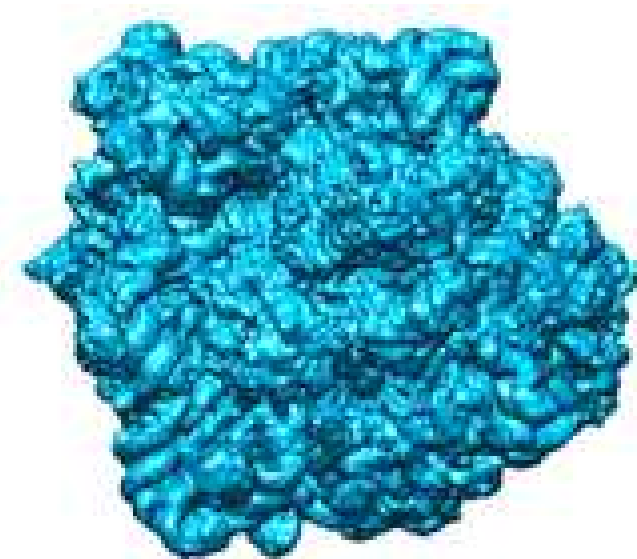
# Evaluation of the quality of a structure

Determining quality of the structure is important to understand reliability of structural details

Unlike MX, no R index is available in electron microscopy to directly compare model and data.

However...

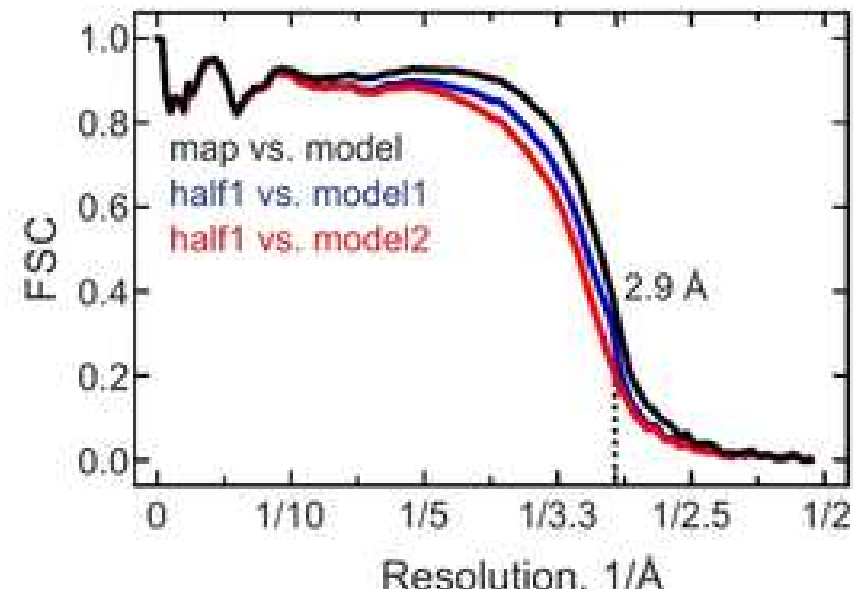
- 1) **Completeness** of the dataset can be evaluated by analysis of orientation frequency of particles



2) **Resolution:** Unlike MX, resolution has to be determined **after** data processing and structure solution

### Fourier Shell Correlation (FSC)

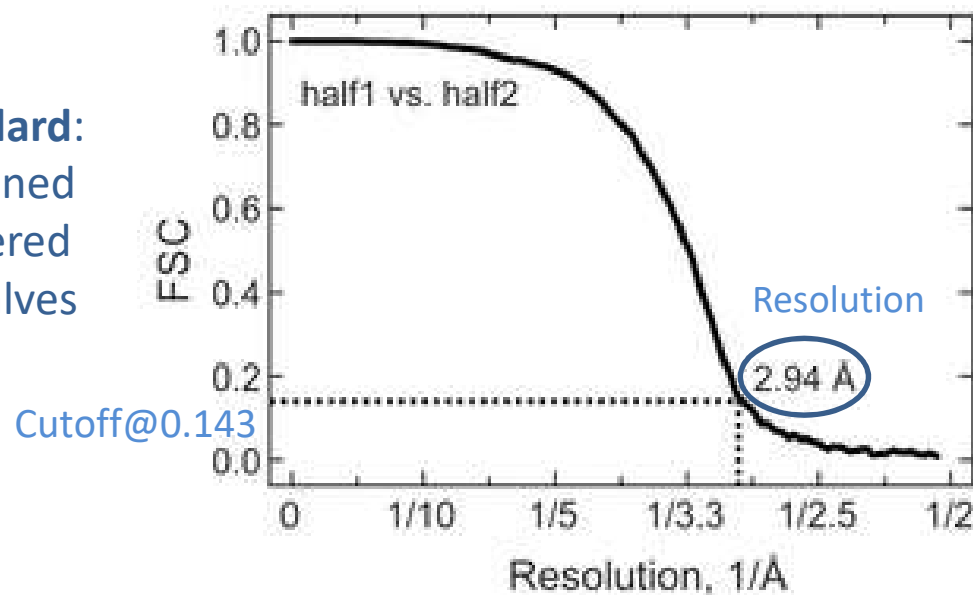
In the Fourier space, cross correlation coefficients are calculated comparing shells of the Fourier space of the model and of the experimental data



### 3) Model bias?

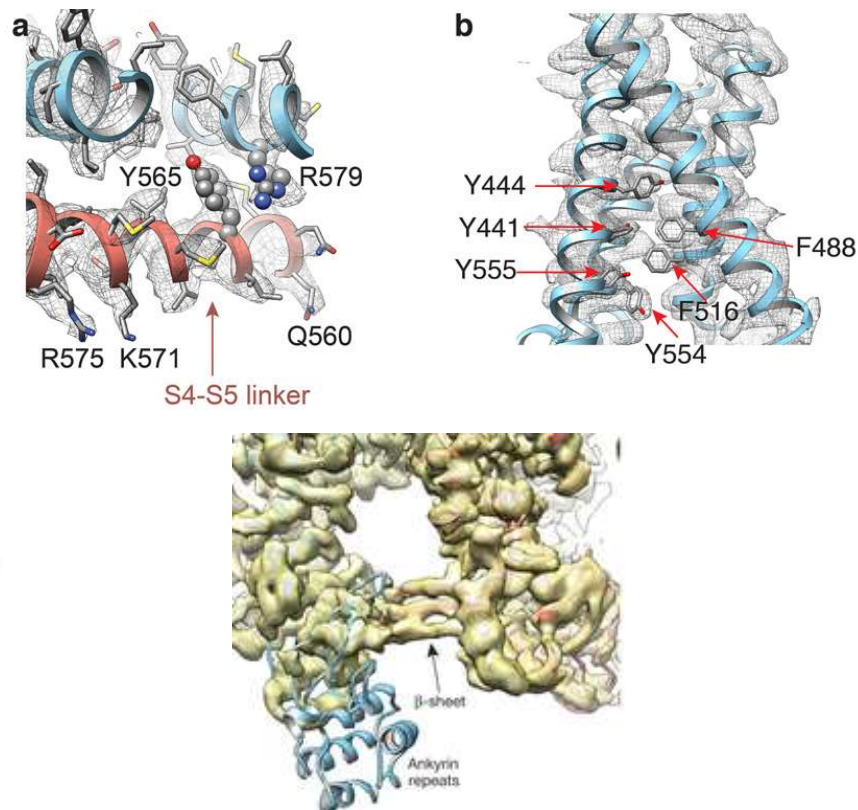
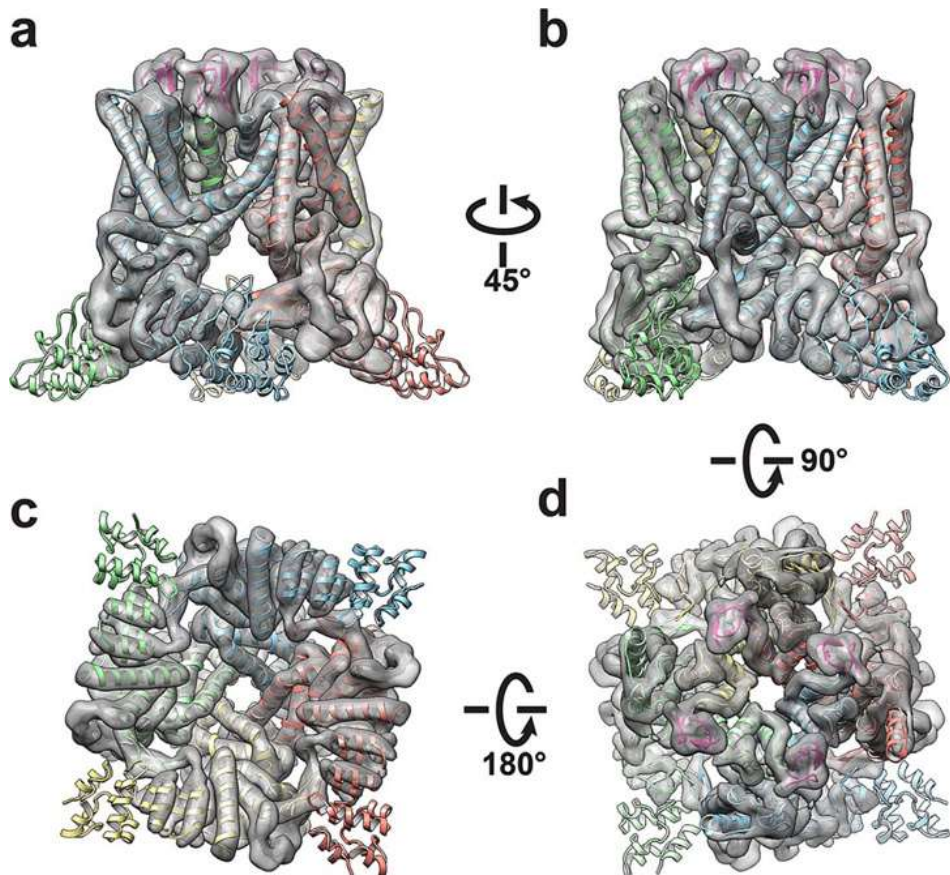
**Fourier Shell Correlation Gold Standard:** dataset is divided in 2, each half refined independently using a low-pass filtered model, FSC calculated between 2 halves

From FSC Gold Standard, resolution can be evaluated...



# Transient Receptor Potential channel

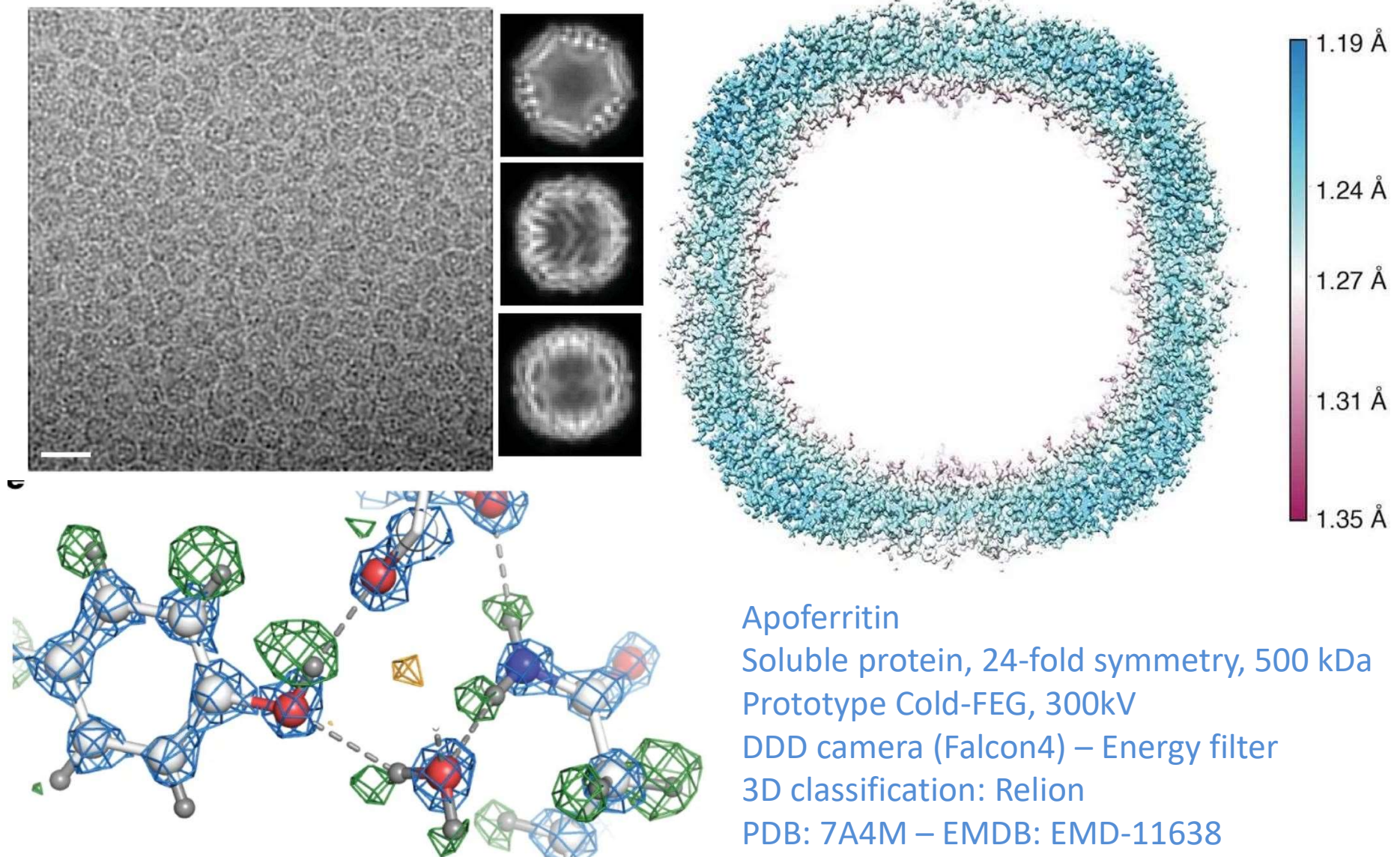
Cheng group (UCSF)  
2013 - 3.2Å resolution



TRPV1  
Membrane protein, 180kDa  
Polara 300kV – DDD camera (K2)  
3D classification Relion

# Apo ferritin

2020 - 1.22 Å resolution

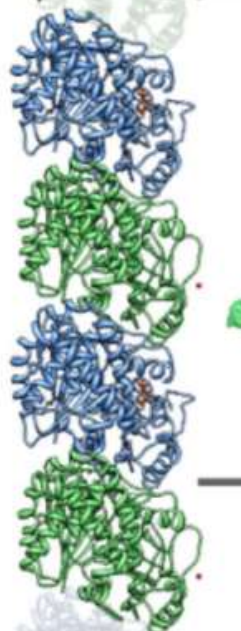


# Microtubule structure and dynamics

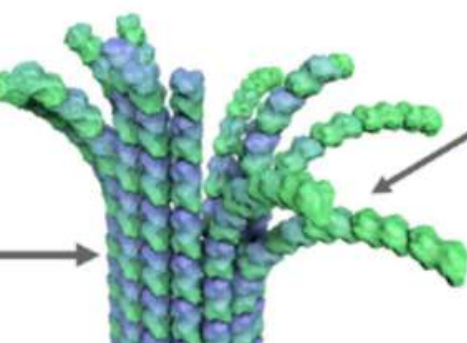
A successful example of an integrative approach to a structural biology problem

1980-1990

**Electron Crystal.**  
Sheets antiparallel protofilaments



Assembly of  $\alpha\beta$ -tubulin dimers is a spontaneous process, while disassembly requires GTP hydrolysis.

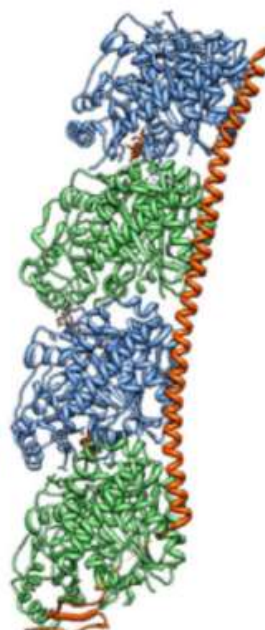


Polymerized Straight

Electron crystallographic structure obtained by non-native sheets, crystallized in presence of Zn.  
X-ray crystal structure obtained with depolymerizing protein.

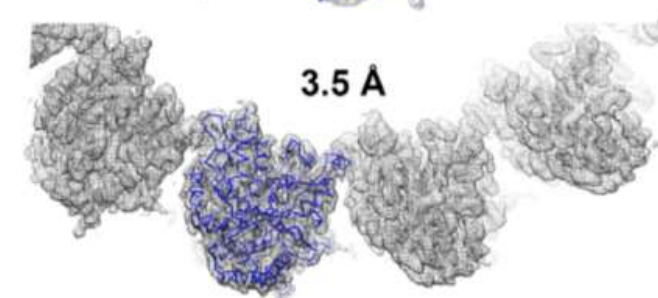
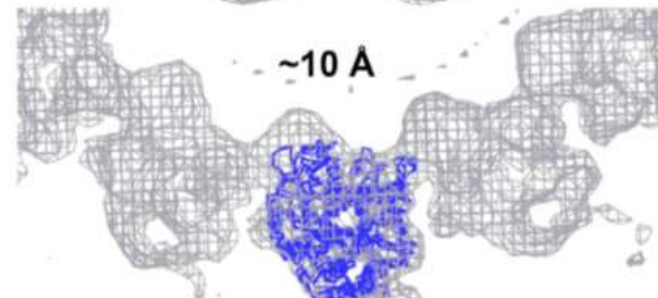
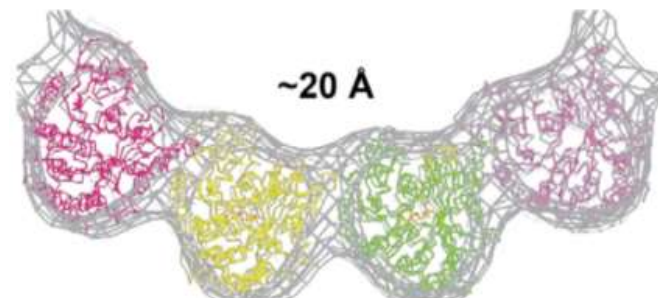
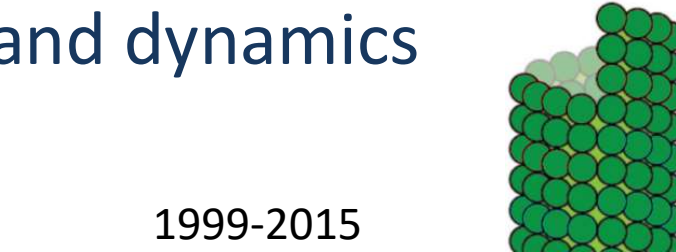
2000

**X-ray Crystal.**  
Dimers bound to depolymerizing proteins



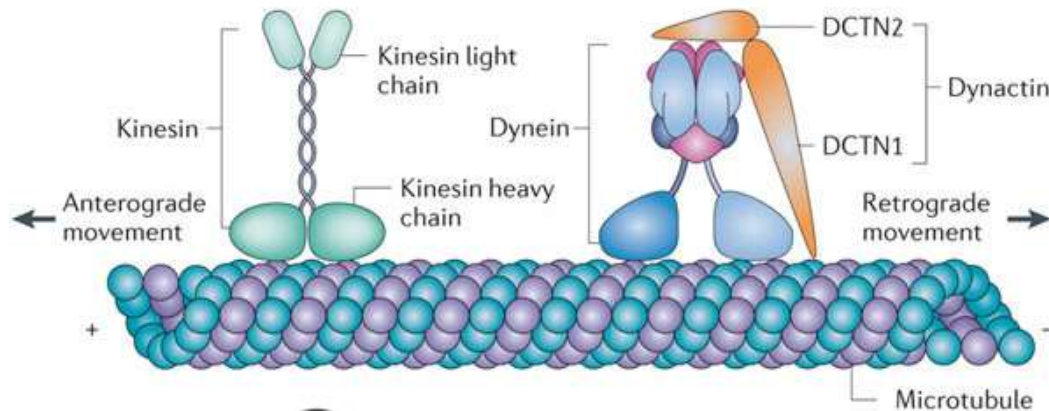
Inhibited Curved

1999-2015



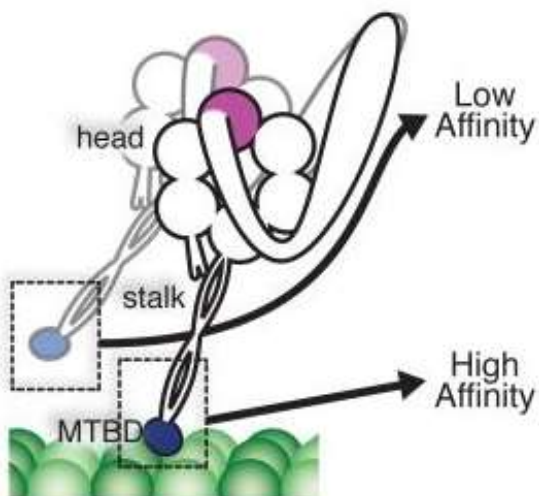
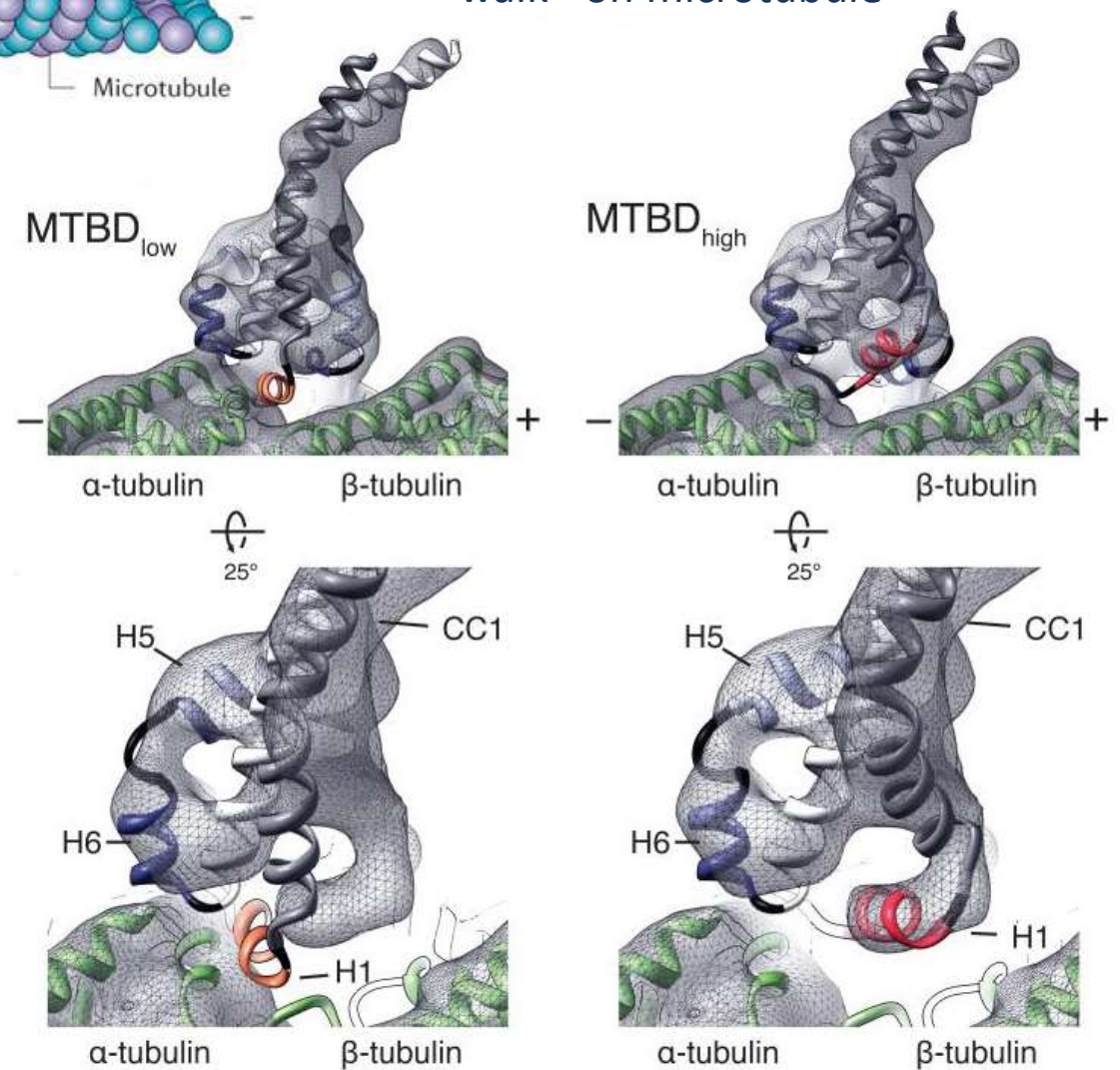
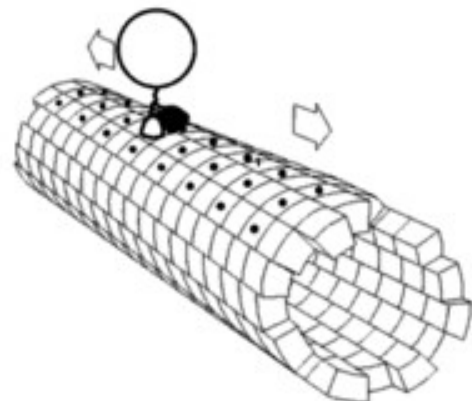
**Single-particle cryo-EM**

Cryo-EM studies on *in vitro* reconstituted microtubules with native conformation.



## Dynein walk

Cryo-EM and X-ray structures of microtubule-dynein complexes allowed to understand mechanism of «dynein walk» on microtubule



# References

- Single-particle electron microscopy: Cheng Y. *et al.*, “A primer to single-particle cryo-electron microscopy.”, **Cell**. **2015**, *161*(3):438-49; De Zorzi R. *et al.*, “Single-particle electron microscopy in the study of membrane protein structure.”, **Microscopy (Oxf)**. **2016**, *65*(1):81-96.
- Relion algorithm: Scheres S.H., “RELiON: implementation of a Bayesian approach to cryo-EM structure determination.”, **J Struct Biol**. **2012**, *180*(3):519-30; Scheres S.H., “A Bayesian view on cryo-EM structure determination.”, **J Mol Biol**. **2012**, *415*(2):406-18.
- Cautionary tales: Henderson R., “Avoiding the pitfalls of single particle cryo-electron microscopy: Einstein from noise.”, **Proc Natl Acad Sci U S A**. **2013**, *110*(45):18037-41; Fan G. *et al.*, “Gating machinery of InsP<sub>3</sub>R channels revealed by electron cryomicroscopy.”, **Nature**. **2015**, *527*(7578):336-41.
- Ryanodine receptor: Cheng Y. *et al.*, “A primer to single-particle cryo-electron microscopy.”, **Cell**. **2015**, *161*(3):438-49; De Zorzi R. *et al.*, “Single-particle electron microscopy in the study of membrane protein structure.”, **Microscopy (Oxf)**. **2016**, *65*(1):81-96.
- TRPV1 channel: Liao M. *et al.*, “Single particle electron cryo-microscopy of a mammalian ion channel.”, **Curr Opin Struct Biol**. **2014**, *27*:1-7; Liao M. *et al.*, “Structure of the TRPV1 ion channel determined by electron cryo-microscopy.”, **Nature**. **2013**, *504*(7478):107-12; Cao E. *et al.*, “TRPV1 structures in distinct conformations reveal activation mechanisms.”, **Nature**. **2013**, *504*(7478):113-18.
- β-Galactosidase: Bartesaghi A. *et al.*, “2.2 Å resolution cryo-EM structure of β-galactosidase in complex with a cell-permeant inhibitor.”, **Science**. **2015**, *348*(6239):1147-51.
- Microtubule: Nogales E., “An electron microscopy journey in the study of microtubule structure and dynamics.”, **Protein Sci**. **2015**, *24*(12):1912-9; Redwine W.B. *et al.*, “Structural basis for microtubule binding and release by dynein.”, **Science**. **2012**, *337*(6101):1532-6.
- Apo ferritin: Nakane T. *et al.*, “Single-particle cryo-EM at atomic resolution.”, **Nature**. **2020**, *587*:152-6.